Revue Roumaine de Chimie, **2009**, *54*(11-12), 1111–1117

Dedicated to the memory of
Professor Ecaterina Ciorănescu-Nenitzescu (1909–2000)

CATALYTIC COMBUSTION OF METHANE OVER UNSUPPORTED AND γ-Al_2O_3 SUPPORTED Sr_2FeTaO_6 and $Sr_2Fe_{0.7}Co_{0.3}TaO_6$ DOUBLE PEROVSKITES

Ionel POPESCU,[*a] Akos REDEY,[b] Ioan-Cezar MARCU,[*a] Bogdan POPESCU,[c] Eva MAKO[d] and Ioan SĂNDULESCU[a]

[a] Department of Chemical Technology and Catalysis, Faculty of Chemistry, University of Bucharest, 4-12 Bd. Elisabeta, 030018 Bucharest, Roumania
[b] University of Pannonia, Faculty of Engineering, Department of Environmental Engineering and Chemical Technology, Veszprem, H-8201, Hungary
[c] National Institute of Materials Physics, 105 bis Atomiştilor Street, Bucharest-Măgurele, P.O. BOX MG-7, code 077125, Roumania
[d] University of Pannonia, Faculty of Engineering, Institute of Materials Engineering, Veszprem, H-8201, Hungary

Received April 27, 2009

Sr_2FeTaO_6 and $Sr_2Fe_{0.7}Co_{0.3}TaO_6$ double perovskites, unsupported and supported on γ-Al_2O_3 were prepared, characterized and studied in the catalytic combustion of methane, as a test reaction for volatile organic compounds (VOCs) destruction. These mixed oxides, with double perovskite structure, present good catalytic activities, and after their dispersion - 5 % (wt.) - on γ-Al_2O_3 support, the reaction rates increased compared with the unsupported samples.

INTRODUCTION

Catalytic combustion is one of the most used technologies for VOCs abatement, due to its definitive character and save of energy.[1-3] Because, as it is known, methane is the most stable hydrocarbon,[4] catalytic combustion of this compound is used as a test reaction for VOCs destruction. Moreover, methane contribution to the greenhouse effect is about 21 times higher than that of carbon dioxide.[5] Anderson et al. early reported that Pd and Pt are good catalysts for methane combustion.[6] Actually it is well known that the noble metals are the most active catalysts for VOCs abatement.[7,8] However, these noble metal catalysts have some disadvantages: they are expensive and easily deactivated at elevated temperatures, due to their volatility and high sintering rate.[9] For these reasons, current research is focusing on the development of metal oxides catalysts that are cheap, stable at high temperatures and active for methane combustion.[10] Perovskites are extensively studied for this purpose due to their thermal stability and low cost.[11-13] On the other hand, the main disadvantage of perovskites is their limited specific surface area[14], but their dispersion on supports may lead to increased exposed surface areas, which can improve their catalytic activity.[15,16] In the present work, we report about results obtained in methane catalytic combustion on unsupported and γ-Al_2O_3-supported Sr_2FeTaO_6 and $Sr_2Fe_{0.7}Co_{0.3}TaO_6$ double perovskites.

RESULTS AND DISCUSSION

a) Catalysts characterization

The XRD patterns of the catalysts are displayed in Fig. 1. The alumina support (Fig. 1a) shows the characteristic reflections of γ-Al_2O_3. For Sr_2FeTaO_6 sample (Fig. 1b) the XRD pattern indicates only the formation of double perovskite

[*] Corresponding authors: ipopescu_unibuc@yahoo.com, marcu.ioan@unibuc.ro

phase, with triclinic symmetry (a = 5.615 Å, b = 5.603 Å and c = 7.912 Å), with no other crystalline compounds.

After dispersion on γ-Al_2O_3, Sr_2FeTaO_6 maintains only partially its structural integrity, the XRD pattern of the supported sample also showing characteristic lines corresponding to the segregated oxides, $SrTa_4O_n$ and δ-Ta_2O_5 (Fig. 1c). No characteristic reflections corresponding to the $SrAl_2O_4$, $FeAl_2O_4$ and $CoAl_2O_4$ spinel phases were found.

The XRD patterns of $Sr_2Fe_{0.7}Co_{0.3}TaO_6$ sample show the characteristic peaks of this double perovskite, but also peaks corresponding to some unidentified phases (Fig. 1d). The attempt to disperse $Sr_2Fe_{0.7}Co_{0.3}TaO_6$ mixed oxide on γ-alumina support, lead to a material having the XRD pattern where only the characteristic peaks of γ-Al_2O_3 were observed (Fig. 1e). This may be due to a high degree of dispersion of the supported phase. .

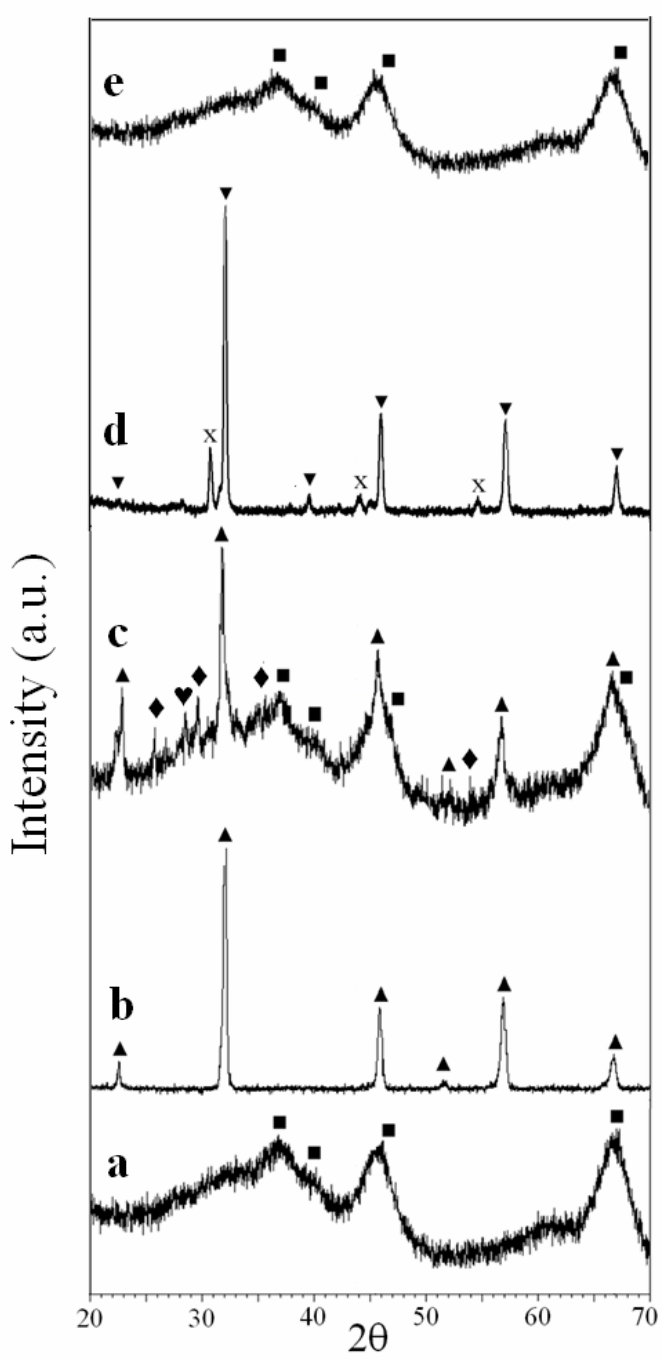

Fig. 1 – XRD patterns of the catalysts: a – γ-Al_2O_3, b – Sr_2FeTaO_6 , c – Sr_2FeTaO_6/Al_2O_3, d – $Sr_2Fe_{0.7}Co_{0.3}TaO_6$, e – $Sr_2Fe_{0.7}Co_{0.3}TaO_6/Al_2O_3$ (■ - γ-Al_2O_3; ▲- Sr_2FeTaO_6; ▼- $Sr_2Fe_{0.7}Co_{0.3}TaO_6$; ♦ - $SrTa_4On$; ♥-δ-Ta_2O_5; x - unidentified phases).

Textural properties of the supported and unsupported samples and of the γ-Al_2O_3 support are summarized in Table 1. The specific surface areas of the unsupported perovskites are low, but usual for perovskite-type oxides, especially for those prepared through solid state reaction. The specific surface areas of the supported samples and of the γ-Al_2O_3 support are very high. The specific surface area of the $Sr_2Fe_{0.7}Co_{0.3}TaO_6/Al_2O_3$ sample is similar to that of the γ-Al_2O_3 support, while the specific surface area of the Sr_2FeTaO_6/Al_2O_3 sample is lower, in line with the observed crystallinity of the samples: higher the crystallinity, lower the specific surface area.

The SEM micrographs for Sr_2FeTaO_6/Al_2O_3 and $Sr_2Fe_{0.7}Co_{0.3}TaO_6/Al_2O_3$ systems are shown in Fig. 2. As it can be observed in the micrograph of Sr_2FeTaO_6/Al_2O_3 sample (Fig. 2a), relatively uniform dispersed islands (bright points) of perovskite, with particle size of 1-10 μm, covers the dark colored surface of alumina support. For $Sr_2Fe_{0.7}Co_{0.3}TaO_6/Al_2O_3$ system, SEM image (Fig. 2b) also shows a relatively uniform dispersion but of smaller particles of perovskite (size < 1μm) in comparison with Sr_2FeTaO_6/Al_2O_3. This accounts for a higher dispersion of the $Sr_2Fe_{0.7}Co_{0.3}TaO_6/Al_2O_3$ sample than the Sr_2FeTaO_6/Al_2O_3 sample.

Table 1

Textural properties of the γ-Al_2O_3 support and of the unsupported and supported mixed oxides.

Sample	BET surface area(m^2/g)	Average pore width (nm)	Pore volume (cm^3/g)
γ-Al_2O_3	192	7.2	0.350
Sr_2FeTaO_6	2.3	9.2	0.008
Sr_2FeTaO_6/Al_2O_3	145	3.2	0.140
$Sr_2Fe_{0.7}Co_{0.3}TaO_6$	1.9	8.7	0.006
$Sr_2Fe_{0.7}Co_{0.3}TaO_6/Al_2O_3$	210	5.2	0.280

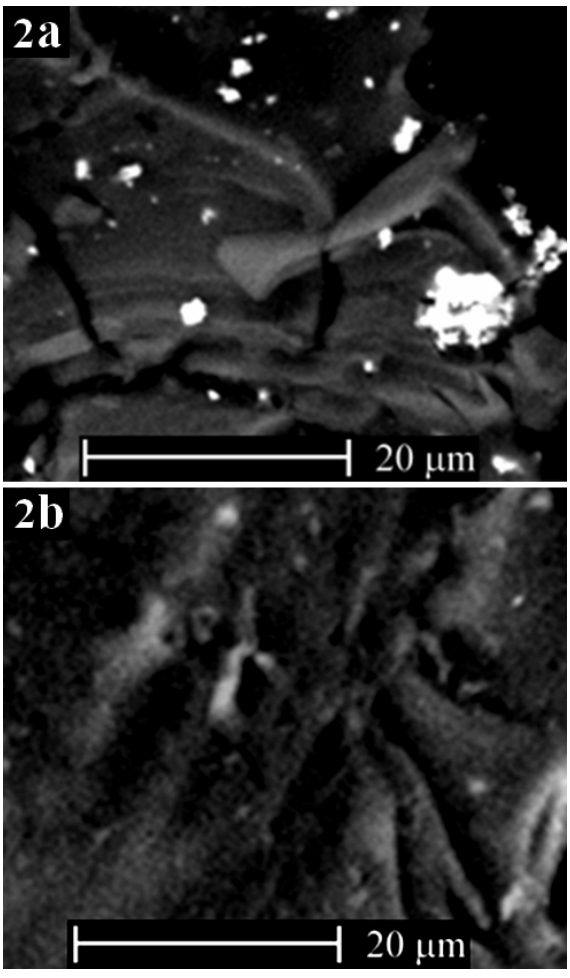

Fig. 2 – SEM micrographs of Sr_2FeTaO_6/Al_2O_3 (a) and $Sr_2Fe_{0.7}Co_{0.3}TaO_6/Al_2O_3$ (b) systems.

b) Catalytic properties

The catalytic activities in methane combustion of unsupported and supported perovskites as well as of the alumina support have been determined in the temperature range of 550-800ºC. The reaction mixture consisted of 5 % methane in air (% vol.), with a VHSV of 16000 h^{-1}. The only reaction product detected on unsupported and supported double perovskites was CO_2, while with γ-Al_2O_3 support a significant amount of CO was found among the products in line with what was reported in Ref.[17]

The results obtained are shown in Fig. 3, where the measured values of methane conversion are plotted as a function of the reaction temperature.

At the same time, the apparent activation energies (E_{act}) corresponding to the transformation on the different catalysts have been calculated (Table 2) from the Arrhenius plots (Fig. 4). The values obtained for the activation energies are comparable with those presented in the literature.[17]

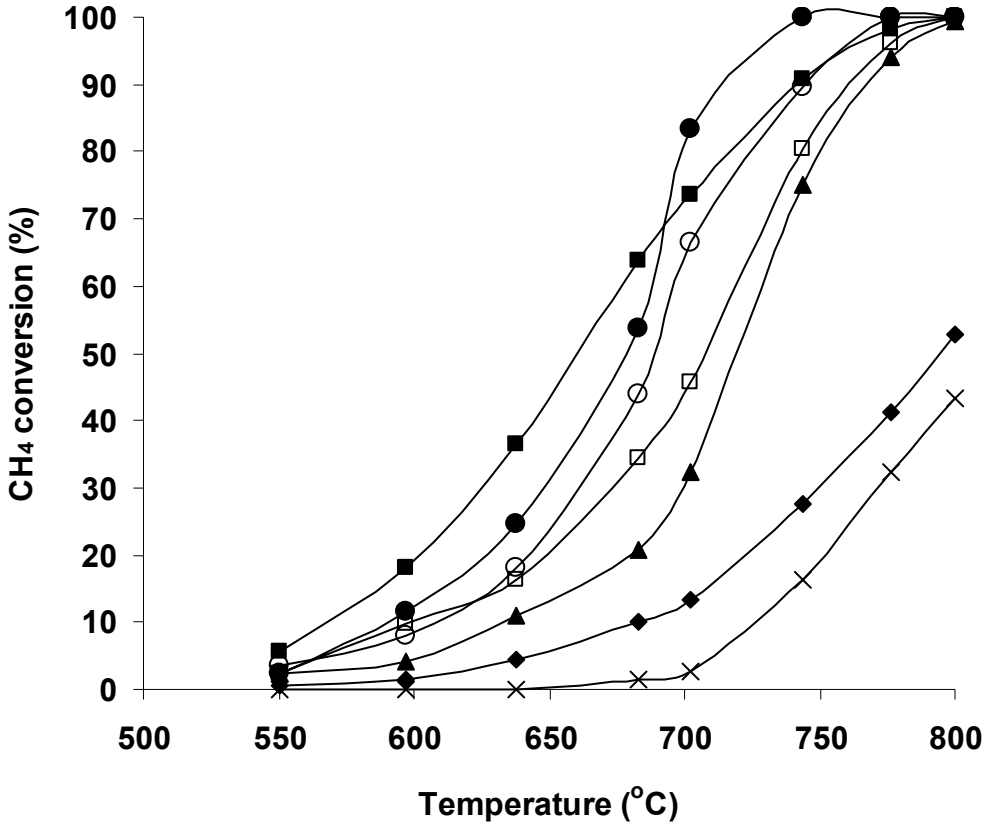

Fig. 3 – Methane conversion versus reaction temperature for (■) Sr_2FeTaO_6, (□) Sr_2FeTaO_6/Al_2O_3, (●) $Sr_2Fe_{0.7}Co_{0.3}TaO_6$, (○)$Sr_2Fe_{0.7}Co_{0.3}TaO_6/Al_2O_3$, (▲) γ-Al_2O_3, (♦) ceramics rings, (x) empty reactor; (VHSV=16000h^{-1}; 5%(vol.) CH_4 in air).

Table 2

Catalytic performances of the catalysts in methane combustion.

Catalyst	T_{50}(°C)	E_{act} (kcal/mol)	Reaction rate at 700°C (x10^5 mol/g·s)	Reaction rate over perovskite phase at 700°C (x10^5 mol/g·s)
γ-Al_2O_3	719	29.9	0.60	-
Sr_2FeTaO_6	659	24.1	0.78	0.78
Sr_2FeTaO_6 / Al_2O_3	707	29.1	0.86	16.57
$Sr_2Fe_{0.7}Co_{0.3}TaO_6$	678	32.7	0.87	0.87
$Sr_2Fe_{0.7}Co_{0.3}TaO_6$/ Al_2O_3	690	29.4	1.25	24.42

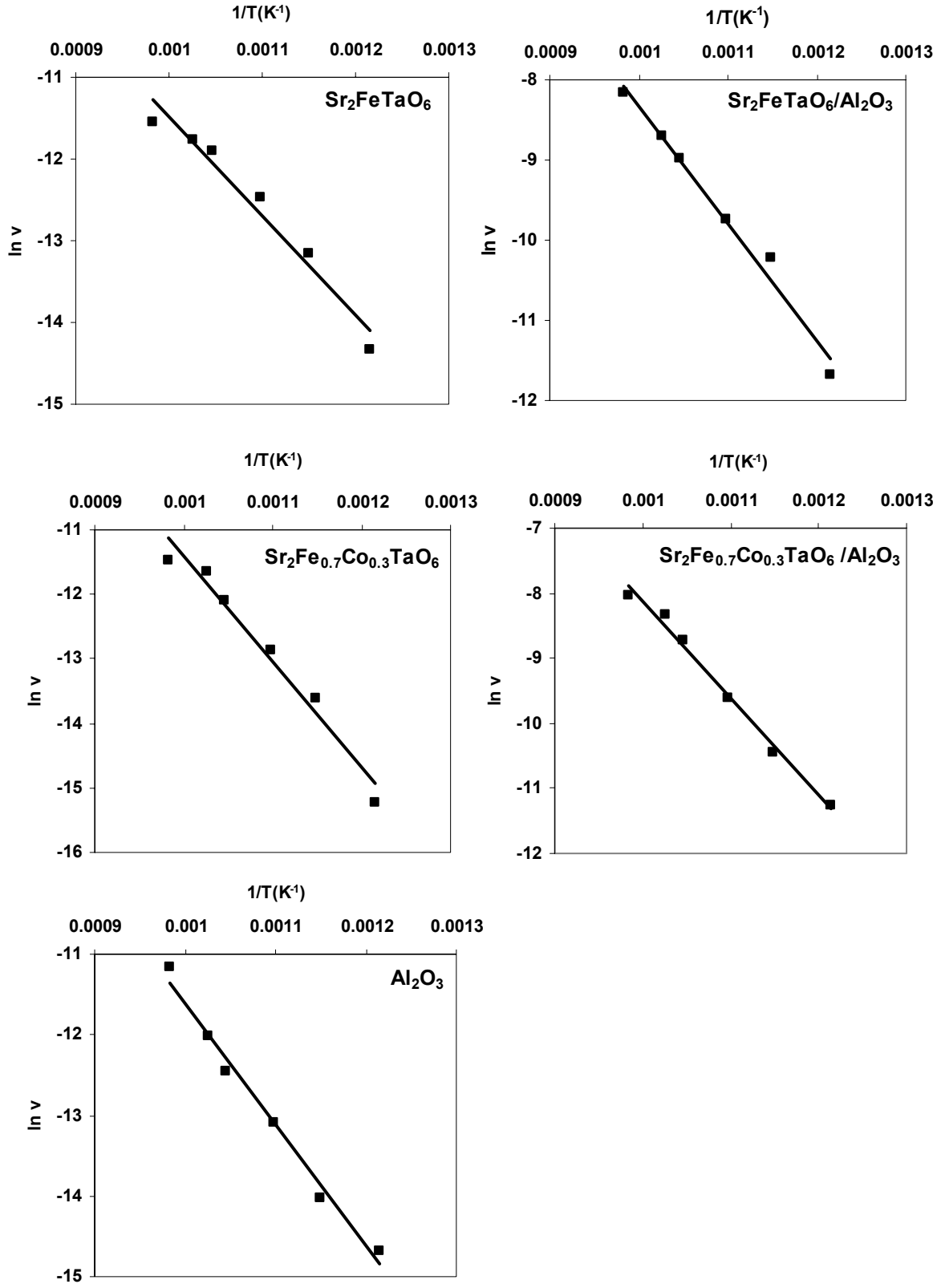

Fig. 4 – Arrhenius plots for methane combustion on the five catalysts.

As clearly shown in Fig. 3 and in Table 2, in terms of T_{50} values (temperature corresponding to 50 % conversion), Sr_2FeTaO_6 perovskite is more active than $Sr_2Fe_{0.7}Co_{0.3}TaO_6$, and both unsupported catalysts are more active than alumina. In terms of the specific activity, for the

reaction at 700ºC, $Sr_2Fe_{0.7}Co_{0.3}TaO_6$ is more active than Sr_2FeTaO_6, and both are more active than alumina. Moreover, both supported catalysts are more active than the corresponding unsupported perovskites.

On the other hand, an important increase of the catalytic activity, expressed as reaction rate per unit mass of active component, was observed after dispersion of the perovskites on γ-Al_2O_3, compared with the unsupported perovskite phases. At the same time, no significant changes of the apparent activation energy of the supported samples with respect to the unsupported ones were observed indicating that no changes of the nature of the active site takes place after dispersion. These observations suggest that dispersion of perovskites on γ-Al_2O_3 results in an increased exposed surface area of the active component, responsible for the observed increase of the catalytic activity.

It should be noted that the specific activity of the active components in the supported catalyst was calculated as the difference between the overall specific activity of the supported catalyst and the contribution of alumina support.

EXPERIMENTAL

a) Catalysts preparation and characterization

The double perovskites Sr_2FeTaO_6 and $Sr_2Fe_{0.7}Co_{0.3}TaO_6$ were prepared by a standard solid state reaction.[18] The mixture of precursors consisted in appropriate amounts of $SrCO_3$, Fe_2O_3, Ta_2O_5 and $Co(CH_3COO)_2{\cdot}4H_2O$, respectively, in order to have the chosen stoichiometric composition. These starting materials were intensively mechanically mixed in an agate mortar, and the double perovskite structure was achieved by calcination at 950ºC for 24 h.

Appropriate amounts of these perovskites were dispersed on γ-alumina, in an attempt to obtain samples with 5 % (wt.) perovskite on the support. The method of dispersion consist in an original procedure, when the very fine grounded particles of perovskite were added in a precursor aqueous solution of $Al(NO_3)_3$, followed by precipitation with ammonia, under intense stirring, at room temperature, up to pH equal to 5.5. The obtained samples were dried at 100ºC for 1 hour. In the end, both systems were calcined under air at 200ºC, 400ºC and 600ºC for 1 hour, and, finally, at 800ºC for 6 hours. All the obtained solids were grounded and sieved to a medium dimension of 0.5 mm before the catalytic test.

The samples structure was investigated by X-ray diffraction (XRD) method. XRD patterns were recorded with a Philips PW 3710 type diffractometer equipped with a Cu Kα source (λ = 1.54 Å), operating at 50 kV and 40 mA. They were recorded over the 20–70° angular range with a 0.02° step and an acquisition time of 1 s per point. Data collection and evaluation were performed with PC-APD 3.6 and PC-Identify 1.0 software.

BET specific surface areas of the samples were measured on a Micromeritics ASAP 2020 system under liquid-nitrogen temperature using N_2 adsorption.

The morphology of the samples and the distribution of the supported oxides have been examined using a Philips XL 30 ESEM (Environmental Scanning Electron Microscope). Accelerating voltage of 20 kV was used. The magnification 100 (M: 100x) allows to obtain the images in a 20 μm scales. The powder samples were fixed on a holder and samples were examined in environmental mode e.g. under the pressure 118 Pa. Then the surface of particle was photographed.

b) Catalytic activity tests

The combustion of methane was carried out in a fixed bed quartz tube down-flow reactor operated at atmospheric pressure. The internal diameter of the reactor tube was 28 mm. The catalyst was supported by quartz wool. The axial temperature profile was measured using an electronic thermometer, placed in a thermowell centered in the catalyst bed. Ceramic rings were used to fill the dead volumes before and after the catalyst bed to minimize potential gas-phase reactions at higher reaction temperatures. The reaction mixture consisted of 5 % (vol.) methane in air. Flow rates were controlled by fine needle valves and were measured by capillary flow-meters. The total volume hourly space velocity (VHSV) was maintained at 16000 h^{-1}.

In a tipical reaction run, the reactor was heated to the desired temperature in the flow of reactants. The system was allowed to stabilize for about 30 min. at the reaction temperature before the first product analysis was made. Each run was carried out over a period of 2-3 hours, until two consecutive analysis were identical. The reaction products were analyzed using a Clarus 500 Gas-Chromatograph equipped with a thermal conductivity detector (TCD), using two packed columns in series (6 ft Hayesep and a 10 ft molecular sieve 5A).

The conversion was calculated as the amount of raw material transformed in reaction divided by the amount that was fed to the reactor. Complete selectivity to CO_2 and H_2O was always observed.

CONCLUSION

Sr_2FeTaO_6 and $Sr_2Fe_{0.7}Co_{0.3}TaO_6$ double perovskites have been obtained by means of the solid state reaction method. The Sr_2FeTaO_6 catalyst is a single perovskite phase, while for $Sr_2Fe_{0.7}Co_{0.3}TaO_6$ sample, XRD patterns also show some unidentified crystalline phases. They exhibit good activity in methane catalytic combustion, $Sr_2Fe_{0.7}Co_{0.3}TaO_6$ being more active than Sr_2FeTaO_6, at higher temperatures ($\geq$ 700°C) and showed almost 100 % conversion of CH_4 to H_2O and CO_2 at around 750°C. Perovskites were supported on γ-Al_2O_3 by incorporation of perovskite powders in the alumina support during its precipitation. Dispersion of these mixed oxides on γ-Al_2O_3, results in an increase of the catalytic activity in the combustion of methane, expressed as reaction rate per unit mass of active component, due to the increasing of the exposed surface area.

Acknowledgment: The authors are grateful to Mr. Oravetz Dezso for his expertise and for technical assistance with scanning electron micrographs recording.

REFERENCES

1. S. Scire, S. Minico, C. Crisafulli, C. Satriano and A. Pistone, *Appl. Catal. B*, **2003**, *40,* 43-49.
2. P. Thevenin, G. Menon and S. Jaras, *CATTECH*, **2003**, *7,* 10.
3. D. Ciuparu, M.R. Lyobovsky, E. Altman, L.D. Pfefferle and A. Datye, *Catal. Rev.*, **2002**, *44,* 593.
4. B. Zongqing, C. Haokan, L. Baoqing and L. Wen, *J. Anal. Appl. Pyrolysis ,* **2005***, 73*, 335-341.
5. E.S. Rubin, R.N. Cooper, R.A. Frosch, T.H. Lee, G. Marlnd, A.H. Rosenfield and D.D. Stine, *Science*, **1992**, *257*, 248.
6. R.B. Anderson, K.C. Stein, J.J. Feenan and L.J. Hofer, *Ind. Eng. Chem*, **1961**, *53*, 809.
7. K. Foger and H. Jaeger, *J. Catal.,***1989**, *120*, 465.
8. R.A. Dalla Betta, *Catal. Today,* **1997***, 35*, 129.
9. R.M. Heck and R.J. Farrauto, "Catalytic Air Pollution Control. Commercial Technology", Van Nostrand Reinhold, New York, 1995.
10. J. Kirchnerova, *Korean. J. Chem. Eng*., **1999**, *16*, 427.
11. L.G. Tejuca, J.L.G. Fierro and J.M.D. Tascon, *Adv. Catal.,* **1989**, *35*, 237.
12. L. Fabrini, A. Kryukov, S. Capelli, G.L. Chiarello, I. Rosetti, C. Oliva and L. Forni, *J. Catal.,***2005***, 232*, 247.
13. I. Popescu, I.-C. Marcu, I. Săndulescu and D. Macovei, *Progr. Catal.,* **2006***,15*, 79.
14. K.Q. Tran, P. Kilpinen and N. Kumar, *Appl. Catal. B*, **2008**, *78,*129-138.
15. M. Alifanti, M. Florea, V. Cortes-Corberan, U. Endruschat, B. Delmon and V.I. Pârvulescu, *Catal. Today,* **2006***, 112*, 169.
16. I. Popescu, A. Urda, T. Yuzhakova, I.-C. Marcu, J. Kovacs and I. Săndulescu, *C. R. Chim*., **2009**, *12*, 1072.
17. S. Cimino, L. Lisi, R. Pirone, G. Russo and M. Turco, *Catal. Today,* **2000***, 59*, 19.
18. M. Raekers, K. Kuepper, H. Hesse, I. Balasz, I. G. Deac, S. Constantinescu, E. Burzo, M. Văleanu and M. Neumann*, J. Optoelectr. Adv. Mater*., **2006**, *8*, 455.